A novel dileucine lysosomal-sorting-signal mediates intracellular EGF-receptor retention independently of protein ubiquitylation

Amy Tsacoumango[1,*], Song Jae Kil[1,*], Liping Ma[1], Frank D. Sönnichsen[1,2,3] and Cathleen Carlin[1,3,4,‡]

[1]Department of Physiology and Biophysics, [2]Cleveland Center for Structural Biology, [3]Case Western Reserve University Cancer Center, School of Medicine, Case Western Reserve University, Cleveland, OH 44106-4970, USA
[4]The Rainbow Center for Childhood PKD at Rainbow Babies and Children's Hospital of Cleveland, 11100 Euclid Avenue, Cleveland, OH 44106, USA

*These authors contributed equally to this work
‡Author for correspondence (e-mail: cathleen.carlin@case.edu)

Accepted 7 June 2005
Journal of Cell Science 118, 3959-3971 Published by The Company of Biologists 2005
doi:10.1242/jcs.02527

Summary

One of the main goals of this study was to understand the relationship between an epidermal growth factor (EGF) receptor dileucine (LL)-motif (679-LL) required for lysosomal sorting and the protein ubiquitin ligase CBL. We show that receptors containing 679-*AA* (di-alanine) substitutions that are defective for ligand-induced degradation nevertheless bind CBL and undergo reversible protein ubiquitylation similar to wild-type receptors. We also demonstrate that 679-LL but not CBL is required for EGF receptor downregulation by an endosomal membrane protein encoded by human adenoviruses that uncouples internalization from post-endocytic sorting to lysosomes. 679-LL is necessary for endosomal retention as well as degradation by the adenovirus protein, and is also transferable to reporter molecules. Using NMR spectroscopy, we show that peptides with wild-type 679-LL or mutant 679-*AA* sequences both exhibit α-helical structural propensities but that this structure is not stable in water. A similar analysis carried out in hydrophobic media showed that the α-helical structure of the wild-type peptide is stabilized by specific interactions mediated by side-chains in both leucine residues. This structure distinguishes 679-LL from other dileucine-based sorting-signals with obligatory amino-terminal acidic residues that are recognized in the form of an extended β or β-like conformation. Taken together, these data show that 679-LL is an α-helical stabilizing motif that regulates a predominant step during lysosomal sorting, involving intracellular retention under both sub-saturating and saturating conditions.

Key words: Adenovirus E3 protein, CBL, EGF receptor, Endosomes, NMR spectroscopy, Protein ubiquitylation

Introduction

Interactions between growth factors and their cognate receptors convey signals from the plasma membrane to the interior of the cell (Schlessinger, 2000). Activated receptors also initiate a series of events leading to their removal from the plasma membrane by endocytosis (Mukherjee et al., 1997). The endocytic machinery controls the cell's capacity to continue signaling by determining whether internalized receptors recycle to the cell surface, or are sent to lysosomes for degradation (Sorkin, 2000). Many growth factor receptors are still active after they are internalized (Baass et al., 1995). Thus endocytosis also influences the nature of the signaling response by controlling access to substrates distributed throughout the cell (Ceresa and Schmid, 2000; Clague and Urbe, 2001; DiFiore and Gill, 1999; Sorkin and Von Zastrow, 2002; Teis and Huber, 2003).

The involvement of endocytosis in cell-signaling is particularly striking in the ERBB family of receptor tyrosine kinases, which includes the epidermal growth factor receptor (EGFR) (Carpenter, 2000; Wiley and Burke, 2001). Ligand-activated EGFRs are recruited to clathrin-coated pits that pinch off from the plasma membrane and subsequently fuse with early endosomes (Wiley, 2003). The majority of endosomal EGFRs are then sorted into the internal vesicles of multivesicular bodies (MVBs) (Miller et al., 1986). MVBs, which originate by budding from early endosomes, mature to form late endosomes capable of fusing with pre-existing lysosomes (Aniento et al., 1996; Futter et al., 1996; Gu et al., 1997). Proteins that are sequestered in MVB internal vesicles are degraded, in contrast to those retained on MVB limiting membranes that recycle back to the plasma membrane (Authier and Chauvet, 1999; Hopkins, 1983). Other ERBB receptors have different trafficking patterns leading to distinct biological outcomes (Baulida et al., 1996; Lenferink et al., 1998; Wang et al., 1999; Waterman et al., 1998; Worthylake et al., 1999). The importance of understanding the relationship between signaling and endocytosis is underscored by the prominence of endocytic sorting abnormalities in human cancers linked to ERBB receptors (Blume-Jensen and Hunter, 2001; Kim and Muller, 1999; Neve et al., 2001).

Endocytic sorting is mediated by signals present in the cytosolic tails of transmembrane protein cargoes (Bonifacino

Table 1. LL-based sorting signals

(a) Consensus dileucine-based sorting signals	
APs	[DE]XXXL[LI]
GGAs	DXXLL
(b) EGFR LL-based motif	
EGFR	673-EAPNQA**LLRIL**-683
ErbB2	705-AMEPNAQMRIL-805
ErbB3	694-EKANKVLARIF-704
ErbB4	703-TAPNQAQLRIL-803
(c) Ad E3-13.7 LL-based motif	
Ad5	81-DRTIAE**LLRIL**-COOH
Ad2	81-DRTIAD**LLRIL**-COOH

(a) Consensus dileucine-based sorting signals (gray box) that bind to AP complexes or GGA proteins (Bonifacino and Traub, 2003).

(b) EGFR juxtamembrane sequences including 679-LL and sequences from the corresponding regions of ErbB2, ErbB3, and ErbB4 (NCBI accession numbers 24571, A36223, and Q15303, respectively).

(c) Carboxyl-terminal sequences from E3-13.7 proteins encoded by group C adenoviruses Ad2 and Ad5 (Hoffman et al., 1992a).

All acidic residues are indicated with a negative charge. The 5-amino acid motif shared by EGFR and E3-13.7 proteins is highlighted by bold.

and Traub, 2003; Bonifacino, 2004; Bonifacino and Dell'Angelica, 1999; Bonifacino and Weissman, 1998). Many of these signals consist of short linear amino acid sequences that may be classified as tyrosine- or dileucine-based because sorting activity is eliminated or reduced when these residues are mutated (Bonifacino and Traub, 2003). The tyrosine-based signals conform to the NPXY or YXXΦ consensus motifs (where X is any amino acid and Φ is a hydrophobic residue) and the dileucine-based signals to [DE]XXXL[LI] or DXXLL (Table 1a). Adaptor molecules that link protein cargoes to the sorting machinery recognize these motifs. Two of these motifs, YXXΦ and [DE]XXXL[LI], are recognized by heterotetrameric adaptor complexes (AP-1, AP-2, AP-3 and AP-4), whereas DXXLL motifs bind GGA adaptor proteins (Bonifacino and Traub, 2003). Several proteins, including clathrin, AP-2 and Dab2, appear to be recognition proteins for NPXY motifs (Bonifacino and Dell'Angelica, 1999). In addition to amino acid motifs, protein ubiquitylation, which may be added to protein cargoes and/or accessory molecules, also facilitates sorting in the endosomal pathway (Bonifacino and Weissman, 1998). Conjugated ubiquitin is recognized by various components of sorting machinery that have consensus ubiquitin-recognition motifs. Equally important are deubibiquitinating enzymes which maintain a sufficient pool of cytosolic ubiquitin for additional protein trafficking (Bonifacino and Weissman, 1998).

Amino acid sorting motifs and protein ubiquitylation are both involved in endocytic EGFR sorting (Wiley, 2003). The EGFR cytosolic tail contains at least three internalization signals, as well as several others implicated in post-endocytic sorting to lysosomes including a 679-LL signal discovered by this laboratory (Kil and Carlin, 2000; Kil et al., 1999). Mutant receptors with 679-*AA* substitutions are delivered to the plasma membrane with normal kinetics, and undergo ligand-induced activation and internalization similar to wild-type receptors. However, in contrast to wild-type receptors that are transported to endocytic compartments where they are protected from in vitro protease digestion, endocytosed mutant receptors remain protease-sensitive and ligand-receptor complexes recycle back to the plasma membrane (Kil and Carlin, 2000; Kil et al., 1999). Although 679-LL is dileucine-based, it lacks other characteristic features of the previously described AP or GGA-binding dileucine-based signals (Table 1b), suggesting a different mode of action.

EGFRs are also downregulated by a 13.7 kDa protein encoded by early transcription region 3 (E3-13.7) of human adenoviruses (Carlin et al., 1989; Hoffman et al., 1990). E3-13.7 is an integral membrane protein with no identified catalytic activity that localizes to early endosomes and MVB limiting membranes (Crooks et al., 2000; Hoffman and Carlin, 1994; Hoffman et al., 1992a). The adenovirus protein diverts receptors in a basal internalization-recycling pathway to MVB internal vesicles without activating EGFR or increasing its internalization rate (Hoffman and Carlin, 1994; Hoffman et al., 1992b). Interestingly, E3-13.7 has an exact copy of a five amino acid sequence including 679-LL found in EGFR that is required for its biological activity (Table 1c), suggesting E3-13.7 can support a normal cellular function (Carlin et al., 1989; Crooks et al., 2000; Hoffman et al., 1992a; Vinogradova et al., 1998). Thus, E3-13.7 provides a novel model for studying the molecular basis of EGFR sorting to lysosomes without ligand-induced saturation of this transport pathway (Piper and Luzio, 2001; Wiley and Burke, 2001).

Protein ubiquitylation has an important role in EGFR membrane trafficking at several sorting steps including internalization and post-endocytic sorting to lysosomes (de Melker et al., 2004; de Melker et al., 2001; Haglund et al., 2002; Levkowitz et al., 1999; Lill et al., 2000). EGFR ubiquitylation is dependent on CBL, a multi-adaptor protein with a RING domain capable of binding a ubiquitin-conjugating enzyme after CBL is recruited to activated receptors and undergoes tyrosine phosphorylation (Bowtell and Langdon, 1995; Joazeiro et al., 1999). Although CBL initially binds EGFR at the plasma membrane, it remains associated with receptors in endocytic compartments including MVB internal vesicles (de Melker et al., 2001; Levkowitz et al., 1999). Recent data suggest ubiquitylated receptors are concentrated in bilayered clathrin coats on endosomal-limiting membranes prior to inward vesiculation to internal vesicles in MVBs (Sachse et al., 2002). Similar to the vacuolar targeting of ubiquitylated cargo proteins in yeast (Amerik et al., 2000; Dupre and Haguenauer-Tsapis, 2001; Katzmann et al., 2001; Losko et al., 2001), however, EGFRs are deubiquitylated before their entry into internal vesicles (Alwan et al., 2003).

The goal of this study was to understand how multiple factors act together to regulate post-endocytic EGFR-sorting to lysosomes in ligand-stimulated cells and in the adenovirus model. This was accomplished by comparing requirements for 679-LL and CBL-dependent EGFR ubiquitylation in both systems. Structures for several functionally diverse leucine-based signals have now been determined (Hurley, 2003). Although most have extended β-sheet conformations, a few are α-helical, providing a basis for understanding recognition of different signals by distinct sets of adaptor proteins. Thus NMR spectroscopy was also carried out to classify the 679-LL signal and to provide a molecular basis for understanding inactivating 679-*AA* substitutions.

Materials and Methods

Antibodies and reagents

The following antibodies were used: anti-adenovirus-E1A-specific antibody (Oncogene Science, Cambridge, MA), E3-13.7-specific peptide antibody produced in rabbits by this laboratory (Hoffman et al., 1990), rabbit anti-CBL antibody (Santa Cruz Biotechnology, Inc., Santa Cruz, CA), mouse anti-human-EGFR monoclonal antibody (Novus Biologicals, Inc., Littleton, CO), rabbit EGFR antiserum (Research Diagnostics, Inc., Flanders, N.J.), rabbit anti-phospho-EGFR (Tyr1045) antiserum (Cell Signaling Technology, Inc., Beverly, MA), mouse human-specific anti-IL2Rα monoclonal antibody (American Type Culture Collection, Rockville, MD), recombinant HRP-conjugated anti-phosphotyrosine antibody (Transduction Laboratories, Lexington, KY), and mouse anti-ubiquitin monoclonal antibody (Berkeley Antibody Co., Richmond, CA). Fluorochrome-conjugated secondary antibodies were purchased from Jackson ImmunoResearch Laboratories, Inc. (Fort Washington, PA), and HRP-conjugated secondary antibodies from Amersham Life Sciences, Inc. (Arlington, IL). Receptor-grade mouse EGF was purchased from Sigma-Aldrich Chemical Co. (St Louis, MO).

Mutagenesis

The Y1045*A* substitution was engineered into a full-length human EGFR cDNA using a mega-primer PCR method to amplify receptor sequences cloned in pBKΔlac^p-CMV (pBKΔlac^p/EGFRwt). pBKΔlac^p-CMV had been generated previously by deleting nucleotides 1098-1305 that encode a lac promoter from the pBK-CMV phagemid (Stratagene Cloning Systems, La Jolla, CA). Two initial PCR reactions were performed using these primer sets: forward primer 5′-GGGGTGACCGTTTGGGAGTTGATG-3′ to anneal to sequences 5′ to a *Bgl*II restriction site at EGFR nucleotide 2951 and reverse mutagenic primer 5′-TTTTGGGAACGGACTGGTTTAT-GGCTTCAGGCACTGGGAGGAAGGTGTC-3′, and forward mutagenic primer 5′-TCCTCCCAGTGCCTGAAGCCATAAACC-AGTCCGTTCCC-3′ and reverse primer 5′-AGGGCTGTCG-AATGTGCTGTTGAC-3′ to anneal to sequences 3′ to a *Hinc*II site at EGFR nucleotide 3627. Each mutagenic primer had a Y1045A substitution (underlined). These reactions generated overlapping products with complementary ends that were allowed to anneal and were amplified using the same forward and reverse primers described above, yielding a 759-bp product with Y1045A that was gel-purified and digested with *Bgl*II and *Hinc*II. The digested PCR product and a 350-bp *Hinc*II-*Xba*I fragment isolated from pBKΔlac^p/EGFRwt were then ligated to pBKΔlac^p/EGFRwt that had been digested with *Bgl*II and *Xba*I. Sequences of all PCR products were verified in their entirety by automated DNA sequencing (Cleveland Genomics, Cleveland, OH).

Plasmids encoding IL2Rα/EGFR chimeras were made using PCR to amplify sequences from human IL2Rα or EGFR cloned in pBKΔlac^p-CMV. Plasmids encoding chimeras with IL2Rα external domains linked to EGFR transmembrane and cytosolic domains truncated to residue Gly-697 were made with the following primers: Forward primer #1 (5′-TGGTGGGGCAGATGGTTTAT-3), complementary to sequences 5′ to a *Bbs*I site at IL2Rα nucleotide 706, and reverse mutagenic primer #2 (5′-TACG*CAGCTG*GTA-CTCTGT TGTAAATA-3′) incorporating a novel *Pvu*II site (in italics) at the 5′ end of the IL2Rα transmembrane domain, and forward mutagenic primer #3 (5′-ACTA**TTTAAA**ATCCCGTCCATCGCC-AC-3′) incorporating a novel *Dra*I site (in bold) at the 3′ end of the EGFR transmembrane domain, and reverse mutagenic primer #4 (5′-ATC*ATCGAT*TTAACCGGAGCCCAGCACTTTG-3′) incorporating an A698Stop (underlined) and a *Cla*I site (in italics) compatible with the pBKΔlac^p-CMV polylinker in EGFR/pBKΔlac^p-CMV. PCR products were gel-purified, digested with novel restriction enzymes at 5′ and 3′ ends, and ligated to pBKΔlac^p-CMV/IL2Rα digested with Bbs I and Cla I. Plasmids encoding chimeras with IL2Rα external and transmembrane domains linked to EGFR cytosolic domains truncated to residue Gly-697 were made with the following primers: Forward primer #1 (listed above), and reverse mutagenic primer #5 (5′-ATA*TTCGAA*GCCCACTCAGGAGGAGGA-3′) incorporating a novel *Bst*BI site (in italics) at the 3′ end of the IL2Rα transmembrane domain, and forward mutagenic primer #6 (5′-GTA**TTCGAA**-GGCGCCACATCGTT-3′) incorporating a novel Bst BI site (in bold) at the 3′ end of the EGFR transmembrane domain, and reverse mutagenic primer #4 (listed above). Plasmids encoding chimeras with IL2Rα external domains, wild-type EGFR cytosolic domains, and transmembrane domains from either EGFR or IL2Rα, were made by ligating a 2529-nucleotide *Dra*III fragment from pBKΔlac^p-CMV/EGFR to plasmids encoding chimeras with a truncated EGFR digested with Dra III. Plasmids encoding chimeras with IL2Rα external domains, EGFR cytosolic domains with 679-*AA*, and transmembrane domains from either EGFR or IL2Rα were made by ligating a 188-nucleotide *Eco*72I-*Eco*RI fragment from pBKΔlac^p-CMV containing an EGFR cDNA with the dialanine substitution (Kil et al., 1999), to plasmids encoding truncated receptor chimeras digested with the same restriction enzymes.

Cell lines

The mouse NR6 cell line is NIH 3T3-derived, lacking endogenous EGFRs (Pruss and Herschman, 1977). Permanent NR6 cell lines expressing wild-type EGFRs, truncated c'-697 receptors, and full-length or truncated EGFRs with a 679-*AA* substitution have already been described (Kil et al., 1999). Permanent cell lines stably expressing Y1045A receptors or IL2Rα/EGFR chimeras were made by transfecting the cells with plasmids described in the previous section using Lipofectin® (GIBCO-BRL, Gaithersburg, MD). Transfected cells were grown in selection-medium containing G418 (0.8 μg/ml Geneticin, GIBCO-BRL) for 10 to 14 days and then enriched for receptor-protein-expression by sterile sorting on a flow-cytometer (Cytofluorograph IIs, Ortho Instruments, Westwood, MA) using monoclonal antibodies to external epitopes. Single cell-derived clones were used in all experiments. All of the cells were maintained in Dulbecco's modified Eagle's medium (DMEM) supplemented with 10% fetal bovine serum (FBS) and 2 mM glutamine.

Metabolic labeling and ^{125}I-EGF cross-linking

Cells were rinsed twice with MEM lacking cysteine and methionine (GIBCO-BRL), and then labeled with ^{35}S-Express Protein Labeling Mix (1175 Ci/mmol, 73% L-[^{35}S]methioine and 22% L-[^{35}S]cysteine, PerkinElmer Life Sciences, Inc., Boston, MA) diluted in the amino-acid-deficient MEM supplemented with 10% dialyzed FBS and 0.2% BSA. The pulse-labeled cells were incubated in chase-medium containing a tenfold excess of nonradioactive cysteine and methionine. The cells were lysed with 1% (w/v) NP-40 in 0.1 M Tris pH 6.8, supplemented with 15% (w/v) glycerol, 2 mM EDTA, and 1 mM EGTA, 0.2 mM phenylmethylsulfonyl fluoride, and 1 μM leupeptin. ^{125}I-EGF cross-linking was carried out as previously described (Kil et al., 1999).

Immunoprecipitation and immunoblotting

Cells were rinsed twice with PBS and lysed with 1% (w/v) NP-40 in a solution of 20 mM Tris pH 7.4, 137 mM NaCl, 10% (w/v) glycerol, 1 mM $MgCl_2$, 1 mM EGTA, 1 mM orthovanadate, 0.1 mM ammonium molybdate, 0.2 mM phenyl arsine oxide, 20 mM β-glycerol phosphate, 20 mM sodium fluoride, 0.2 mM phenylmethylsulfonyl fluoride, and 1 μM leupeptin. The lysis buffer was supplemented with 5 mM N-ethylmaleimide in experiments to detect EGFR ubiquitylation, to minimize the action of deubiquitylating enzymes during cell harvest. The lysates were incubated with primary antibody

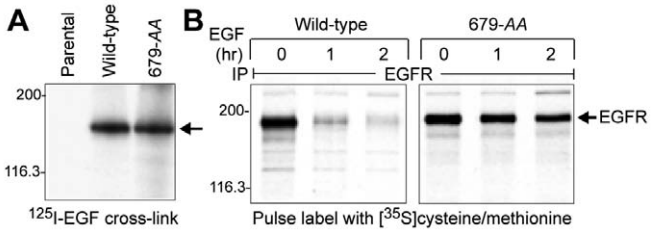

Fig. 1. (A) Parental NR6 cells that lack endogenous EGFRs and NR6 cell lines stably expressing wild-type human EGFR or a mutant receptor with an inactivating 679-*AA* substitution, were incubated with ^{125}I-EGF for 2 hours at 4°C, followed by incubation with a chemical cross-linker at room temperature for 15 minutes. (B) NR6 cell lines expressing wild-type or 679-*AA*-mutant receptors were pulse-labeled with a mixture of [^{35}S]cysteine and [^{35}S]methionine for 30 minutes followed by a 3-hour incubation in chase medium. The pulse-labeled cells were then stimulated with EGF for 0, 1 or 2 hours and cell lysates were immunoprecipitated with a human EGFR-specific antibody. Equal aliquots of total cellular protein (A) or EGFR immunoprecipitates (B) were resolved by SDS-PAGE for autoradiographic detection. Molecular mass standards: 200,000 Da (myosin); 116,300 Da (β-galactosidase).

for 1 hour and then with an aliquot of protein A-Sepharose CL-4B beads (Sigma-Aldrich) for an additional 90 minutes, at 4°C on a rotating platform. Immunoprecipitates were washed five times with lysis buffer, resolved by SDS-PAGE and transferred to nitrocellulose membranes (Laemmli, 1970; Towbin et al., 1979). Membranes were blocked with 5% dry milk dissolved in TBS-T (10 mM Tris pH 7.4, 150 mM NaCl, 0.1% Tween 20), and incubated with primary antibodies diluted in blocking solution overnight at 4°C. Blots to be probed with the ubiquitin antibody were blocked with TBS-T supplemented with 5% dry milk and 1% BSA. Blots were washed and incubated with HRP-conjugated secondary antibodies diluted in blocking solution for 1 hour at room temperature, followed by detection using ECL (Amersham Life Sciences). Acrylamide gels with radioactive samples were treated with En^{3}Hance (New England Nuclear) for fluorography.

Confocal microscopy

Cells grown on poly-L-lysine-coated glass coverslips were permeabilized with 0.5% (w/v) β-escin in a solution of 80 mM PIPES pH 6.8, supplemented with 5 mM EGTA and 1 mM $MgCl_2$, for 5 min and then fixed with 3% (v/v) paraformaldehyde-PBS pH 7.4, for 15 minutes. Cells were stained with primary antibodies or fluorophore-conjugated secondary reagents for 1 hour or 30 minutes, respectively, at 37°C. Antibodies were diluted with PBS containing 0.5% β-escin and 3% RIA-grade BSA, and cells were pre-incubated with PBS-0.5% β-escin supplemented with 5% normal serum from the host animal used to generate secondary antibodies to block non-specific binding. Cells were examined with a Zeiss LSM 410 scanning laser confocal microscope (Zeiss, Göttingen, Germany) using the 488/568-nm wavelength lines of an argon-krypton laser. Image resolution using a Zeiss 100× Plan-Neofluor oil objective and Zeiss LSM software was 512 × 512 pixels.

Adenovirus infections

Adenovirus stocks were grown in human embryonic-kidney-293 cells, and titers were determined by plaque assay, using standard techniques. Adenoviruses that either overproduce the E3-13.7 protein or that have an internal deletion in the E3-13.7 open reading frame, have been

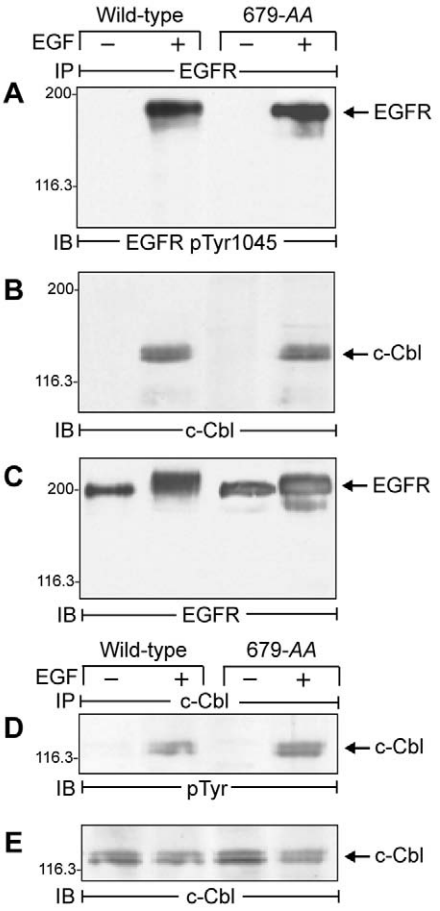

Fig. 2. (A-E) Wild-type and 679-AA-mutant cells were lysed and lysates from unstimulated (–) cells and from cells stimulated with EGF for 10 minutes (+) were immunoprecipitated with antibodies against (A-C) human EGFR or (D,E) CBL. Immunoprecipitates were transferred to nitrocellulose filters for immunoblotting after SDS-PAGE. EGFR immunoprecipitates were divided in half and resolved on two gels. One filter was incubated with a phosphorylation-specific EGFR (pTyr1045) antibody (A), and the second with a CBL antibody (B). The filter in (B) was re-probed with an EGFR antibody as a loading control (C). (D,E) The filter with CBL immunoprecipitates was incubated with a phosphotyrosine-specific antibody (pTyr) (D), and then re-probed with a CBL antibody as a loading control (E). IP, immunoprecipitation; IB, immunoblot. Molecular size in Da on the left.

described elsewhere (Carlin et al., 1989). Cells were acutely infected with approximately 200 plaque-forming units per cell according to established protocols (Hoffman and Carlin, 1994).

NMR sample preparation and spectroscopy

A synthetic peptide corresponding to EGFR residues Ser671 to Phe688 was purchased from Peninsula Laboratories, Inc. (San Carlos, CA). A similar peptide containing a 679-*AA* substitution was synthesized by standard solid-phase peptide synthesis using Fmoc-chemistry on a MilliGen 9050 PepSynthesizer (Bedford, MA). The NH_2-terminus of the mutant peptide was manually acetylated following the last deprotection procedure, yielding C-terminal amides. Peptide was purified by reversed-phase HPLC using a semi-preparative C8 column (Grace Vydac, Hesperia, CA) after it was cleaved from TGR resin (Novabiochem, San Diego, CA). Peptide

identity was confirmed by MALDI-TOF mass spectrometry and NMR spectroscopy. Solution-state NMR samples were made by dissolving 2 to 3 mg lyophilized peptide in 500 μl of H_2O containing 10% D_2O, corresponding to a final peptide concentration of 2 to 4 mM. The pH of aqueous samples was adjusted to 5.2 to 5.8. Perdeuterated dodecyl phosphocholine (DPC, Cambridge Isotope Laboratories, Andover, MA) was added to aqueous solutions (final concentration=120 to 210 mM) for data acquisition in the presence of detergent micelles. Paramagnetic spin-labeled experiments were carried out with 5-doxyl stearic acid (0.4 to 1 mM, diluted from a 40 mM stock in 30% DPC, Sigma-Aldrich).

NMR experiments were performed on Varian INOVA 500 MHz and 600 MHz spectrometers equipped with *z*-axis pulsed-field gradient, triple-resonance probes. The following experiments were executed for most of the samples: one-dimensional-^{1}H spectroscopy, total-correlation spectroscopy (TOCSY) with mixing times of 35 or 65 milliseconds and a 10 kHz dipsi-2 spin-lock field, nuclear-Overhauser-effect spectroscopy (NOESY), and double-quantum filtered-correlation spectroscopy (DQF-COSY). Rotating-frame nuclear-Overhauser-effect-spectroscopy measurements (ROESY) were also acquired for aqueous samples. Solvent suppression was accomplished using a 1.5-millisecond pre-saturation pulse or the Watergate-pulse sequence (Piotto et al., 1992). Several mixing times (50, 150, 200 and 300 milliseconds) were used in 2D-NOESY experiments with micelle samples. The 2D-NMR spectra were collected with 16 or 32 transients per t1 in 256×1k complex data points. The data were processed with VNMR software (Varian, Palo Alto, CA) on a SGI workstation, using cosine-apodization functions in both dimensions, and zero-filling to a final data size of 1k×1k. Shifts are reported as chemical shift deviations (CSDs), where CSDs= experimental shift–random coil value (Andersen and Tong, 1997), with DSS (sodium 2,2-dimethyl-2-silapentane-5-sulfonate) used as the shift-standard throughout.

Image preparation

All digital images were prepared using Adobe Photoshop® 6.0 and Adobe Illustrator® CS software packages from Adobe Systems Incorporated (San Jose, CA).

Results

Validation of cell models

Experiments were carried out in EGFR-null mouse-NR6 cells, engineered to express human EGFRs under the control of a CMV promoter. Cells were used that had been transfected with plasmids encoding either wild-type EGFRs or receptors with a 679-*AA* substitution previously shown to disrupt post-endocytic sorting to lysosomes (Kil and Carlin, 2000; Kil et al., 1999). Cell lines isolated by single-cell cloning were selected for stable human receptor expression using fluorescence-activated cell sorting and a species-specific anti-human-EGFR antibody. We used cell lines with moderate amounts of surface EGFR to minimize saturation of transport pathways associated with extremely high receptor densities (Wiley, 1988). Results were also verified in at least three independent cell lines for each receptor construct. Fig. 1A, showing ^{125}I-EGF cross-linking results, verifies that the parental NR6 cells lack endogenous receptors, and that the stable cell lines used in this study express similar levels of human receptors on the cell surface. Experiments shown in Fig. 1B were carried out after cells had been incubated for 30 minutes with a mixture of [^{35}S]-labeled cysteine and methionine, followed by a 3-hour chase with an excess of non-radioactive amino acids such that a majority of pulse-labeled receptors was delivered to the plasma membrane (Kil et al., 1999). The radiolabeled cells were then incubated with EGF, and cell lysates were immunoprecipitated with an EGFR antibody to determine plasma-membrane-receptor stability as a function of ligand-induced intracellular trafficking. This analysis, which showed that pulse-labeled 679-*AA* receptors were only modestly reduced in cells incubated with EGF for two hours – in contrast to wild-type receptors where the majority was degraded during the first hour of EGF treatment – confirms the trafficking-phenotype exhibited by these mutant receptors (Kil and Carlin, 2000; Kil et al., 1999).

Wild-type and 679-*AA* EGFRs both form ligand-inducible molecular complexes with CBL that persists in early endosomes

Although CBL binds activated EGFRs through several different mechanisms (Lefkowitz et al., 1999; Smit et al., 1996), direct binding to phospho-Tyr1045 is required for sorting of EGFR to lysosomes (Grovdal et al., 2004). Thus, we first tested whether 679-*AA* receptors are capable of directly binding CBL, using a phosphorylated-Tyr1045-specific anti-EGFR antibody. This antibody detected 679-*AA* receptors isolated from EGF-stimulated cells on immunoblots, suggesting that activated 679-*AA* receptors possess CBL-docking sites similar to the wild-type molecule (Fig. 2A). We then determined whether activated 679-*AA* receptors interact with CBL using several approaches. First, receptor-protein complexes were immunoprecipitated from unstimulated or EGF-treated cells, and receptor-associated proteins were analyzed by immunoblotting with a CBL-specific antibody. This experiment showed that CBL forms a stable complex with ligand-activated 679-*AA* receptors, similar to wild-type receptors (Fig. 2B). Second, we determined whether CBL is a substrate for activated 679-*AA* receptors by examining immunoprecipitates of CBL with a phosphotyrosine-specific antibody. This experiment demonstrated that EGF treatment resulted in tyrosine phosphorylation of CBL in cell lines that either express 679-*AA* or wild-type receptors (Fig. 2D). Finally, cells were co-stained with antibodies against EGFR and CBL to establish whether CBL was associated with 679-*AA* receptors in early endosomes – as reported for wild-type receptors (de Melker et al., 2001; Levkowitz et al., 1999). Fig. 3 shows that, in unstimulated cells expressing either of the receptors, EGFR and CBL were predominantly found on the plasma membrane and in the cytosol, respectively. Approximately 10 minutes after the addition of EGF, wild-type and 679-*AA* receptors redistributed to punctate intracellular vesicles, consistent with their uptake from plasma membrane. The majority of intracellular wild-type and 679-*AA* receptors colocalized with CBL, which was presumably recruited to activated receptors from the cytosol pool. We have previously reported that, following a similar period of EGF treatment, wild-type and 679-*AA* receptors both colocalize with vesicular transferrin receptors but not with Lamp-1, consistent with the internalization of activated receptors to early endosomes (Kil and Carlin, 2000). Together with the data present here, we conclude that wild-type and 679-*AA* receptors both form complexes with the CBL multi-adaptor protein that persists in early endosomes.

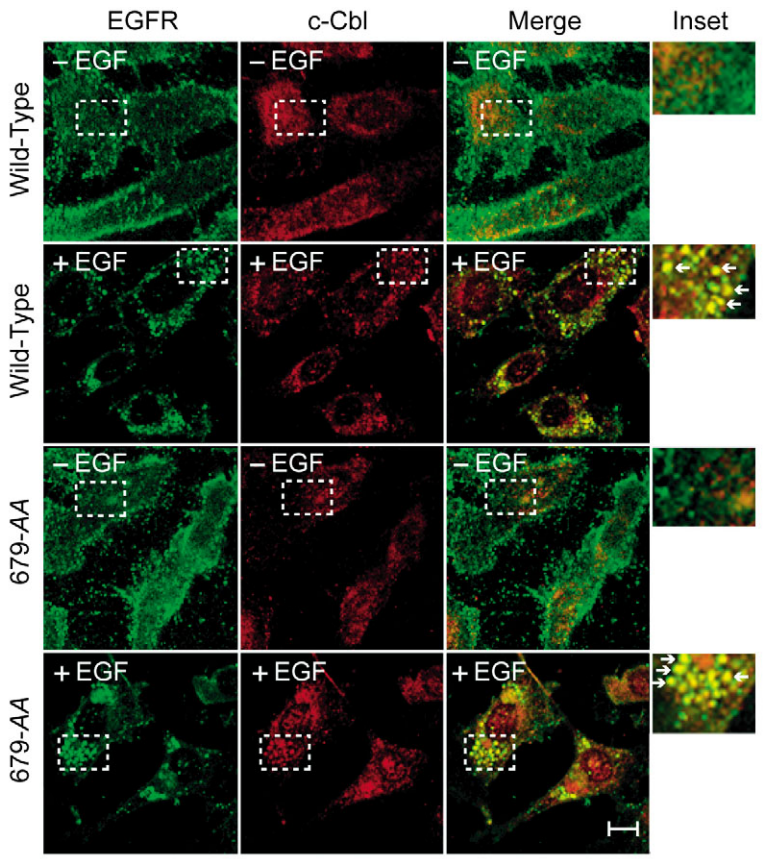

Fig. 3. Confocal images of permeabilized cells that were unstimulated (– EGF) or stimulated with EGF (+ EGF) and co-stained with antibodies against EGFR (green channel) and to CBL (red channel). Green and red channels were merged after both fluorescent signals were adjusted to similar levels. The yellow color indicates the overlap of red and green fluorescence. Areas corresponding to the enlarged insets shown on the extreme right are boxed in all of the panels. Some intracellular vesicles co-stained for EGFR and CBL are highlighted with arrows. Bar, 10 μm.

679-*AA* EGFRs undergo ligand-dependent ubiquitylation

We next determined whether 679-*AA* receptors are targets for protein ubiquitylation, by immunoblotting EGFR immunoprecipitates, isolated from unstimulated cells or cells treated with EGF, with a ubiquitin-specific antibody. This analysis demonstrated that wild-type and 679-*AA* receptors were both ubiquitylated within a few minutes of ligand stimulation (Fig. 4A). Ubiquitylation was also evident in the increased molecular weight of the modified receptors (Fig. 4A,B) and the formation of a protein-ladder, characteristic of substrates with multiple ubiquitin targets (Fig. 4A) (Hershko and Ciechanover, 1998). Together with data from the previous section, showing that CBL interacts with 679-*AA* receptors, these results suggest that the mutant receptors are targets for CBL-mediated ubiquitylation, similarly to wild-type EGFR. We also observed that receptor ubiquitylation was transient in both cell lines (Fig. 4A). Although receptor degradation can account for some loss of ubiquitylated wild-type receptors, this cannot explain transient ubiquitylation observed for the mutant receptors, which we have shown previously recycle to the plasma membrane following ligand-induced internalization (Kil and Carlin, 2000; Kil et al., 1999). The simplest explanation for these data is that ubiquitylated 679-*AA* receptors are substrates for deubiquitylating enzymes (DUBs) in early endosomes similar to what has been reported for wild-type receptors (Alwan et al., 2003).

Molecular requirements for EGFR downregulation by E3-13.7 adenovirus protein

Cells expressing wild-type or 679-*AA* receptors were infected with adenovirus to determine whether 679-LL is necessary for E3-13.7-mediated downregulation of EGFR. Two different adenovirus stocks were used, one encoding an intact E3 transcription region and another with an internal deletion in the E3-13.7 gene that renders it defective for EGFR downregulation (Hoffman et al., 1992a; Hoffman et al., 1992b). NR6-derived cell lines expressed similar levels of early E1A viral proteins following infection with equal amounts of plaque-forming units of either virus (Fig. 5A), but E3-13.7-related proteins only if cells are infected with adenovirus containing an intact E3 region (Fig. 5B). EGFR-protein stability was measured in infected cells after they had been pulse-labeled for 15 minutes with [^{35}S]-amino-acids. Thirty minutes after cells were switched to non-radioactive chase medium, wild-type and 679-*AA* receptors both exhibited a mobility shift, which was expected because of the N-linked oligosaccharide content of the EGFR (Carlin and Knowles, 1984). Pulse-labeled wild-type receptors disappeared within three hours in cells that had been infected with the E3-13.7-positive virus (Fig. 5C). This is consistent with previous results showing an EGFR half-life of approximately 3 hours in NR6 cells previously infected with a

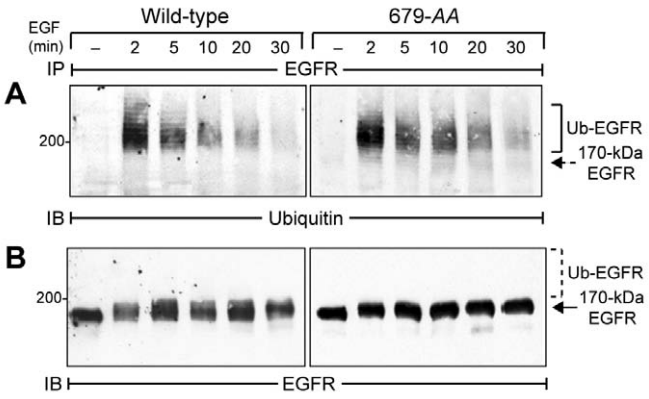

Fig. 4. (A) Cell lines expressing wild-type or 679-*AA*-mutant receptors were stimulated with EGF for the times indicated. EGFR immunoprecipitates resolved on a 5% acrylamide gel were transferred to nitrocellulose filters and immunoblotted with a ubiquitin-specific antibody. Solid-line brackets indicate location of ubiquitylated EGFR (high molecular mass), arrow indicates 170-kDa EGFR (non-ubiquitylated). (B) The filter in (A) was re-probed with an EGFR-specific antibody. Arrow indicates 170-kDa EGFR (non-ubiquitylated). High molecular mass ubiquitylated EGFR (dashed-line bracket) was not seen unless the film was overexposed (data not shown).

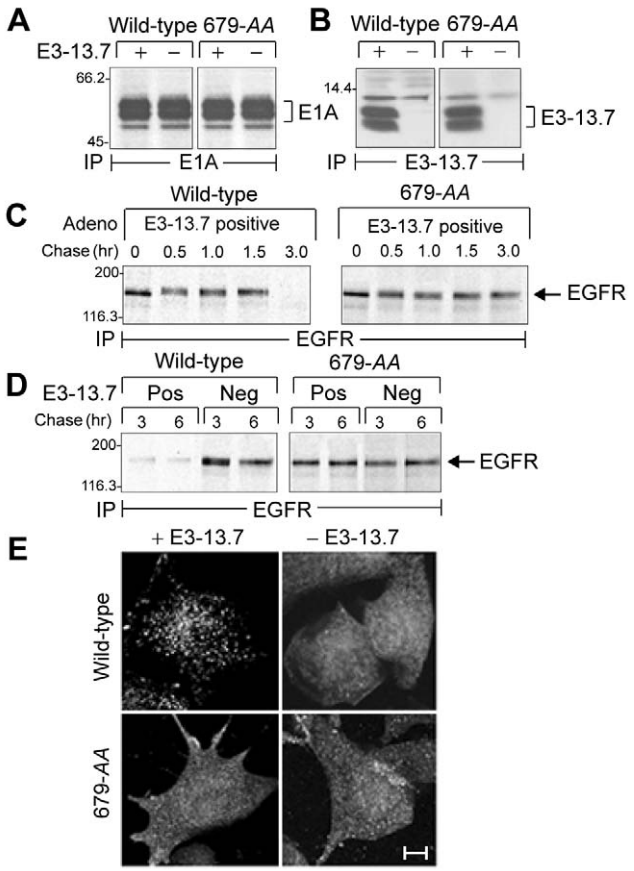

Fig. 5. (A,B) Cells infected with E3-13.7-positive (+) or E3-13.7-negative (–) adenoviruses were labeled with a mixture of [^{35}S]cysteine and [^{35}S]methionine for 3 hours, and cell lysates were immunoprecipitated with antibodies against E1A (A) or E3-13.7 (B) early adenovirus proteins. (C,D) Adenovirus-infected cells were pulse-labeled for 15 minutes at 16 hours post-infection and were then switched to chase-medium for up to 3 hours (C) or 6 hours (D). Cell lysates were immunoprecipitated with an anti-EGFR antibody. Immunoprecipitates in panels A-D were resolved by SDS-PAGE for autoradiographic detection of radiolabeled proteins. Molecular mass standards: 66,200 (BSA); 45,000 (ovalbumin); 14,400 (lysosyme). (E) Confocal images of permeabilized cells that had been infected with E3-13.7-positive (+ E3-13.7) or E3-13.7-negative (– E3-13.7) adenoviruses and stained with an EGFR-specific antibody. Pos, positive; neg, negative. Bar, 10 μm.

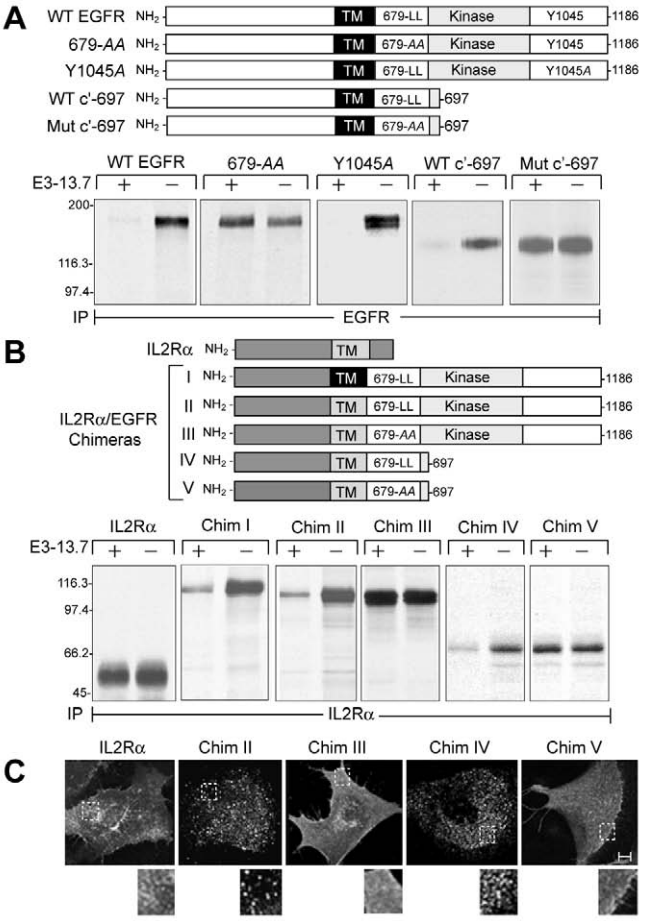

Fig. 6. (A,B) Permanent cell lines stably expressing EGFR-related proteins (A) or IL2Rα-EGFR chimeras (B), whose genotypes are depicted schematically at the top of each panel, were infected with E3-13.7-positive (+) or E3-13.7-negative (–) adenoviruses. The infected cells were pulse-labeled with a mixture of [^{35}S]cysteine and [^{35}S]methionine for 30 minutes followed by a 5-hour incubation period in chase-medium. Cell lysates were immunoprecipitated with antibodies against external epitopes of EGFR (A) or IL2Rα (B). Immunoprecipitates were resolved by SDS-PAGE for autoradiographic detection of radiolabeled proteins. (C) Confocal images of permeabilized cells that had been infected with the E3-13.7-positive adenovirus and stained with an IL2Rα-specific antibody. Areas corresponding to the enlarged insets shown beneath each image are boxed in all of the panels. Bar, 10 μm. TM, transmembrane; 679-LL and 679-*AA*, wild-type and mutationally inactivated lysosomal sorting-signals, respectively.

E3-13.7-positive virus compared with more than 20 hours in cells infected with the E3-13.7-negative virus (Crooks et al., 2000). The rapid downregulation of newly synthesized receptors also suggests that E3-13.7 may re-route receptors to lysosomes from the secretory pathway as well as post-endocytically. By contrast, 679-*AA* receptor expression levels remained constant for as long as six hours after the switch to non-radioactive chase medium (Fig. 5C,D), showing that 679-LL is obligatory for E3-13.7-induced EGFR degradation. These results were verified in at least three independent cell lines for each receptor construct (data not shown).

Wild-type and 679-*AA* receptor localization in infected cells was also evaluated by confocal microscopy. As shown previously, wild-type receptors accumulated in intracellular vesicles before E3-13.7-induced degradation (Crooks et al., 2000; Hoffman and Carlin, 1994; Hoffman et al., 1992b), in contrast to cells infected with the E3-13.7-negative virus, where wild-type receptors remain associated with the plasma membrane (Fig. 5E). The 679-*AA* receptors, however, were predominantly associated with the plasma membrane in cells infected with E3-13.7-positive or E3-13.7-negative viruses (Fig. 5E). Thus, the 679-LL EGFR signal is required for E3-13.7-dependent intracellular retention as well as degradation. This is in contrast to results seen shortly after cells are treated with EGF (see, for example Fig. 3), where both receptors accumulate in early endosomes because activated 679-*AA* and

wild-type receptors exhibit similar rates of accelerated internalization (Kil and Carlin, 2000; Kil et al., 1999).

Additional experiments were carried out to evaluate a potential role for CBL during E3-13.7-induced receptor trafficking. This adaptor protein interacts with EGFR by two mechanisms one, mentioned already, involving direct binding to phosphorylated-Tyr1045 and the second through Grb2-CBL complexes recruited to the EGFR C-terminus (Marmor and Yarden, 2004). Previous results show that kinase-inactive K721*A* receptors are degraded similarly to wild-type receptors, which is consistent with the idea that autophosphorylated docking sites are dispensible for E3-13.7-mediated downregulation (Hoffman and Carlin, 1994). It is nevertheless possible that E3-13.7 activates these sites by another mechanism. Thus, cells expressing Y1045*A* receptors with a defective CBL docking site or receptors truncated up to residue Gly697 (c'-697 receptors), which eliminates the intrinsic kinase domain and all known phosphotyrosine docking sites (illustrated in top panel of Fig. 6A), were infected with E3-13.7-positive and -negative viruses. Pulse-chase experiments showed that all of these receptor proteins were synthesized the same in cells expressing either virus (data not shown). Protein-stability was assessed by comparing the abundance of radioactive EGFR in infected cells pulse-labeled with [^{35}S]-amino-acids for 30 minutes followed by a 5-hour chase in non-radioactive medium. Receptor proteins were significantly reduced in cells expressing E3-13.7 compared with cells infected with the E3-13.7-negative virus. An exception were c'-697-receptors or full-length-receptors with a mutated 679-*AA* signal, which each had similar levels in both sets of infected cells (Fig. 6A). In addition, wild-type EGFRs were not ubiquitylated in adenovirus-infected cells (data not shown). These findings therefore suggest that CBL is not required for E3-13.7-induced downregulation, in contrast to the 679-LL signal, which is obligatory.

679-LL is part of a dominant, autonomous lysosomal sorting-signal in adenovirus-infected cells

Cells expressing protein chimeras that contain cytoplasmic sequences of the EGFR fused to extracellular sequences of the IL2 receptor α subunit (IL2Rα) were infected with E3-13.7-positive and -negative adenoviruses to test whether 679-LL sorting function is transferable to other molecules. IL2Rα sequences were used because IL2Rα is usually not expressed in fibroblasts (Lando et al., 1983), and wild-type IL2Rα is not a target for E3-13.7-mediated downregulation (Fig. 6B). Chimeras containing the transmembrane domains from each of the parental molecules were produced, and in all chimeras each domain was intact and derived from IL2Rα or EGFR. In all the chimeras containing a wild-type 679-LL signal, the stability of pulse-labeled protein chimeras was greatly reduced in cells infected with an E3-13.7-positive virus, compared with cells infected with the negative control virus (Fig. 6B). This included chimeras with transmembrane domains from IL2Rα (Chimera II) and those with a truncated (Chimera IV) or full-length EGFR cytoplasmic domain (Chimeras I and II). The only chimeras where expression was not reduced had inactivating 679-*AA* substitutions in an intact EGFR cytoplasmic tail (Chimera III) or a truncated tail lacking a catalytic domain and C-terminus (Chimera V). Cell lines that express some of the chimeras had been infected with adenovirus and were also examined by confocal microscopy. Chimeras with EGFR-sequences containing a wild-type 679-LL motif concentrated in punctate

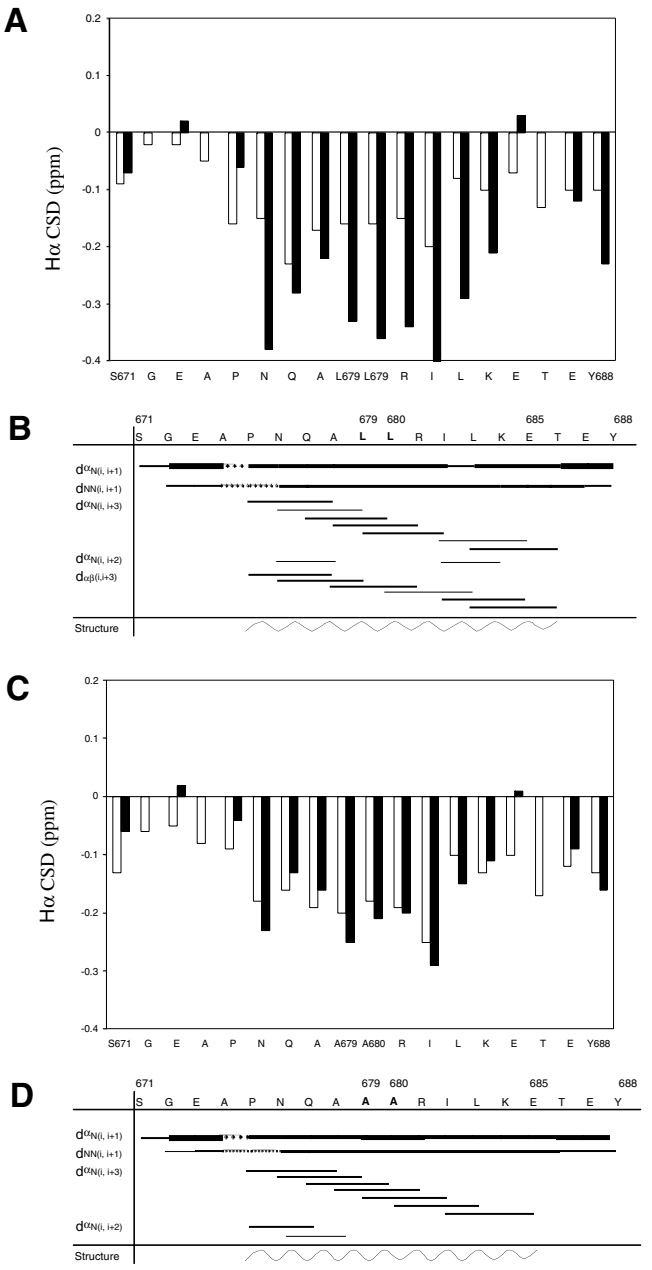

Fig. 7. (A,C) The Hα CSDs for synthetic peptides with (A) 679-LL or (C) 679-*AA* sequences where a value of 0 corresponds to random coil. CSDs are represented as ppm on the *x*-axis [ppm=(shift observed/oscillator frequency)×10^6]. Positive and negative values represent upfield and downfield shifts, respectively. Amino acid residues are labeled on the *y*-axis, based on the published human EGFR sequence (NCBI accession number P00533). Data were obtained for peptides dissolved in water (open bars) or in the presence of DPC micelles (black bars) at 5°C. (B,D) Summary of intramolecular NOEs observed for (B) wild-type and (D) mutant peptides in the presence of DPC micelles. NOE-intensity-strength is indicated by the thickness of the lines. Dotted lines indicate proline CδH-proton resonance effects.

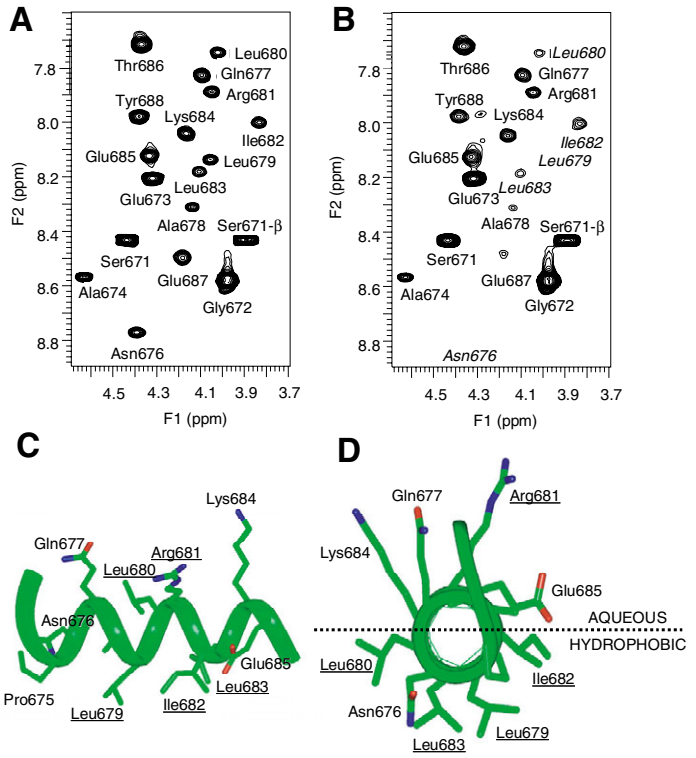

Fig. 8. (A,B) 2D-TOCSY proton spectra for residues Ser671 to Tyr688 in DPC-micelle-bound state (A) without and (B) with a 5-doxyl stearic acid spin-label. Italicized residues in (B) exhibit line-broadening due to the spin label. F1, amide protons; F2, Hα protons. (C,D) Representation of the predicted orientation of DPC-micelle-stabilized helical structure as a (C) side or (D) front view. EGFR residues also occurring in the adenovirus E3-13.7 protein are underlined. Red and blue residues represent oxygen and nitrogen, respectively, in amino acid side-chains.

intracellular vesicles in cells infected with the E3-13.7-positive virus (Chim II and Chim IV in Fig. 6C) This was in contrast to IL2Rα parental molecules or chimeras with a mutated 679-*AA* motif (Chim III and Chim V in Fig. 6C) that were predominantly localized to the plasma membrane. These data indicate that 679-LL promotes intracellular retention independently of EGFR sequences outside the juxtamembrane region, and that it is an autonomous signal that can be transferred to other molecules in the E3-13.7 trafficking model.

679-LL side-chains are crucial secondary-structure determinants

Secondary-structure determinations provide valuable insights into binding properties of intrinsic sorting-signals (Hurley et al., 2002). Although we had, based on computer modeling, already predicted that 679-LL resides in an amphipathic helix (Kil et al., 1999), the inactivating alanine substitutions had little effect on the overall secondary structure when using the same algorithms. We thus hypothesized that leucine side-chains interact with other elements in the cellular environment to stabilize a nascent amphipathic helix. This hypothesis was tested using NMR spectroscopy where the conformational properties for EGFR residues Ser671 to Tyr688 with wild-type 679-LL or mutant 679-*AA* sequences were compared. Data were collected in two different solvents, water and DPC micelles. DPC is a zwitterionic detergent capable of stabilizing secondary structures characteristic of proteins that bind membrane lipids or hydrophobic pockets in other molecules (Lauterwein et al., 1979). Thus, this approach allowed us to ask two related questions. First, do DPC micelles induce a stable helical structure? Second, what is the contribution of the crucial leucine residues to DPC-induced structure?

Unambiguous chemical-shift assignments were made for Hα protons in all of the residues in the wild-type peptide using a variety of NMR experiments (see Materials and Methods). The experimentally derived chemical shifts were then compared to random coil-value predictions by calculating chemical-shift deviations (CSDs). CSDs may be used to predict protein secondary structures, because Hα protons of all 20 naturally-occurring amino acids experience an upfield shift of >0.1 ppm with respect to random coil-values when in a helical configuration, and a comparable downfield shift in a β-strand-extended configuration (Wishart et al., 1992). Upfield chemical shifts consistent with helical secondary structure were obtained for residues Asn676 to Tyr688 in the wild-type peptide (open bars in Fig. 7A). Several other data, however, suggested that this helical conformation is not stable in water (data not shown). First, the only cross-peaks observed in ROESY and NOESY spectra were those expected for intra-residue- and sequential-backbone-connectivities. Second, the phi-angle-dependent NH-CαH vicinal-coupling constants extracted from 1D proton or 2D DQF-COSY spectra fell within the range of 6-8 Hz, consistent with conformational averaging of the backbone. Third, NOE patterns, indicative of short distances characteristic of a stable α-helical secondary structure [i.e. dαN(i,i+3) or dβN(i,i+3)], were not detected. The CSDs for these residues, however, were significantly enhanced by the addition of DPC micelles, indicative of direct interactions between this region of the peptide and the micelle surface (open bars in Fig. 7A). In addition, this region had six dαN(i,i+3) NOEs out of a total of eight possible NOEs, consistent with medium-range intramolecular interactions in a helical structure that were analysed in the presence of DPC micelles (Fig. 7B). Altogether, these data suggest that 679-LL resides in a nascent helical structure, stabilized by direct interactions with DPC micelles.

Data obtained for the peptide with a 679-*AA* mutation are summarized in Fig. 7C-D. The mutant peptide exhibited structural properties characteristic of a flexible nascent helix, and CSDs in water were nearly indistinguishable from those of the wild-type peptide (open bars in Fig. 7C). However, although the mutant peptide had in the presence of DPC micelles the same pattern of long-range NOEs as the wild-type peptide (Fig. 7D), the magnitude of upfield CSDs induced by micelles was less pronounced compared with data for the wild-type peptide (black bars in Fig. 7C). Thus, we conclude that, 679-*AA* does not disrupt the inherent secondary structural properties of this region, but the nascent helix containing these inactivating substitutions is not as well stabilized by micelle interactions as the wild-type signal.

679-LL orientation in the DPC micelle solvent

Data in Fig. 7 indicate that, the larger hydrophobic side-chains in both of the leucine residues necessary for EGFR

downregulation play an important role in micelle binding. We tested this hypothesis by adding a micelle-integrating spin-label to determine the positioning of the wild-type peptide relative to the micelle interior (Lindberg et al., 2003). This approach permits identification of key residues necessary for helix-stabilizing micelle-interactions because their resonance fingerprints will be affected by the presence of the spin label. Fig. 8 shows the upfield region of 2D-TOCSY spectra for the wild-type peptide in DPC-micelle-medium in the absence (Fig. 8A) or presence (Fig. 8B) of spin label. The resonance for some residues either completely disappeared (Asn676 and Leu679) or was substantially reduced (Leu683, Leu680 and Ile682) in the presence of the spin label. Several other residues experienced little to no change in this experiment, indicating a larger spatial separation from the spin-label in the micelle interior. These included Lys684, Thr686 and Gly672, which also displayed additional exchange cross-peaks between water and amide-protons in NOESY spectra (not shown). Altogether, these results suggest that residues Asn676 to Glu685 form an amphipathic helix at a water-micelle-interface (Fig. 8C-D). The hydrophobic side of the helix, including 679-LL, interacts with the micelle surface and the hydrophilic side of the helix is oriented towards the aqueous environment. The side-chains of the two key leucine residues are largely buried in the micelle surface. We have reported previously that the corresponding LL sequence in the E3-13.7 protein exhibits similar micelle-binding and helical properties (Vinogradova et al., 1998). Interestingly, the 679-LL-stabilized helical structure represented in Fig. 8 includes all the other conserved residues that are also found in the E3-13.7 protein (underlined in Fig. 8D).

Discussion

Membrane-protein sorting is regulated by intrinsic amino acid motifs and by protein ubiquitylation. The data presented in this study provide insight into how these mechanisms contribute to the sorting of EGFR to lysosomes. We had reported previously that receptors with a 679-*AA* mutation undergo ligand-induced activation and have an increased rate of internalization, similar to wild-type receptors (Kil et al., 1999). Once internalized, the mutant receptors diverge from the normal sorting pathway leading to lysosomes and recycle back to the plasma membrane (Kil et al., 1999). We had also reported that the E3-13.7 adenovirus protein induces EGFR degradation by diverting constitutively recycling receptors to lysosomes (Hoffman and Carlin, 1994; Crooks et al., 2000). The current findings extend these observations in several significant ways. First, the mutant receptors form ligand-induced complexes with CBL and undergo reversible protein ubiquitylation, similar to wild-type receptors. Second, the 679-LL signal is necessary for intracellular retention, leading to degradation of EGFR-related molecules or protein chimeras induced by the adenovirus protein. Third, peptides with 679-LL and 679-*AA* residues have the same overall secondary α-helical propensity, but 679-LL confers increased binding to membrane-mimetic micelles. Taken together, these data show that 679-LL regulates a predominant step during lysosomal sorting under both sub-saturating and saturating conditions and might be recognized in an α-helical conformation.

The best-studied dileucine-based sorting motifs also have crucial N-terminal acidic residues that are not found in EGFR or E3-13.7. These dileucine signals bind two different classes of clathrin adaptors, the GGA proteins and the heterotetrameric AP-protein complexes (see Table 1a) (Bonifacino, 2004). The acidic residue in DXXLL-type motifs undergoes hydrogen-bonding necessary to maintain these signals in an extended β or β-like conformation, which is needed to bind to VHS domains in GGA proteins. Similarly, YXXO signals bind to the μ2 subunit of AP-2 in an extended conformation. This conformation is advantageous because it allows the maximum exposure of binding-determinants within a short amino-acid-motif to the surface of a cognate binding-module. Acidic residues are also important for LL-binding to APs, but at position –4 [D/E]XXXLL instead of position –3 (Bonifacino and Traub, 2003). Several [D/E]XXXLL-type signals have been identified that lack this acidic residue but which have a phosphorylatable N-terminal Ser/Thr residue, capable of increasing AP-dependent sorting-efficiency in its phosphorylated state (Bonifacino and Traub, 2003). Although these requirements are not met in EGFR, residue Thr83 in E3-13.7 is a potential casein kinase 2 substrate and would therefore conform to a regulatable AP-binding site (Table 1c). We cannot exclude the possibility that this residue is transiently modified under certain physiological conditions, even though Thr83 phosphorylation has never been detected (Hoffman et al., 1992a). We have demonstrated that the E3-13.7 cytosolic tail binds clathrin APs in vitro (N. Cianciola and C.C., unpublished data). However, AP-binding depends on an N-terminal YXXΦ motif and not the LL motif (N. Cianciola and C.C., unpublished data). We therefore conclude that the signal shared by the EGFR and the E3-13.7 protein has additional binding-activities not yet ascribed to other dileucine-based sorting-signals.

Data presented here suggest that 679-LL is recognized as part of an amphipathic α-helix. Compared to the extended conformations of acidic cluster LL motifs that bind GGAs, there are far fewer cases of interactive proteins that bind α-helical-recognition motifs. Ca^{2+}-calmodulin, which wraps around helical binding domains in target proteins, is probably the best-known example in this category (Crivici and Ikura, 1995). It has recently been shown that the LD class of leucine-based signals, which were originally identified in the paxillin superfamily and mediate binding to compact four-helix bundles comprising focal adhesion targeting (FAT) domains, have a similar α-helical structure (Hoellerer et al., 2003). Given its proximity to the membrane, it is conceivable that 679-LL sorting activity is regulated by reversible binding to biological membranes. We also found that the structural properties of the entire juxtamembrane region, including 679-LL, are strongly influenced by micelle mimetics of biological membrane (Choowongkomon et al., 2005). Alternatively, recent crystal structure of the tyrosine kinase domain supports hydrophobic interactions between this region and the amino-terminal lobe of the tyrosine kinase domain (Stamos et al., 2002). The crystal structure also shows that Arg681 projects into solvent (Stamos et al., 2002), suggesting it mediates protein-protein interactions through hydrogen-bonds. Both possibilities are consistent with a recently published model, proposing that ligand-binding is coupled to rotation of the transmembrane helices resulting in reorientation of the cytoplasmic domains within receptor dimers, trans-autophosphorylation and stimulation of

enzymatic activity (Fleishman et al., 2002). This rotation-activation-model predicts that juxtamembrane domain-conformation is dynamically regulated during intracellular trafficking associated with receptor activation.

Although it is not currently known how the adenovirus protein interacts with 679-LL in unoccupied receptors, there are several possibilities that are not mutually exclusive. First, the viral protein might immobilize and/or concentrate a 679-LL-interactive partner at the endosomal membrane to either restrict its range of action or to provide a reservoir of the factor for slow-release. Second, the viral protein might protect a 679-LL-interactive partner from proteolytic degradation, thereby prolonging its action. Third, the viral protein might compete for factors that normally mask 679-LL, preventing recognition of unoccupied receptors by the lysosomal sorting machinery. These three possibilities would each result in a more effective presentation of an interactive partner, necessary for lysosomal sorting to 679-LL. Fourth, the corresponding signal in the viral protein, which is known to be required for its EGFR downregulatory function (Hilgendorf et al., 2003), might sequester a 679-LL-interactive partner necessary for EGFR recycling, causing sorting to lysosomes by default. However, this possibility is not supported by data from ligand-stimulated cells, which show that 679-*AA* receptors recycle after they are internalized (Kil and Carlin, 2000).

If 679-LL is the predominant signal that regulates lysosomal sorting, what is its role in protein ubiquitylation? Comparison of trafficking requirements during ligand- and adenovirus-induced downregulation provides novel insight to this question. Protein ubiquitylation is required to sequester activated EGFRs in clathrin-coated microdomains on MVB-limiting membranes after ligand-induced internalization (Sachse et al., 2002). However, EGFRs exit these microdomains before they are packaged into inwardly invaginating vesicles (Sachse et al., 2002), suggesting additional mechanisms might be needed to continue sorting towards lysosomes. Evidence from the adenovirus model demonstrates that 679-LL facilitates intracellular retention of constitutively internalized EGFRs followed by degradation. Thus, ubiquitin-dependent MVB-sub-domains might act as dynamic reservoirs to accommodate a rapid increase of activated receptors in this compartment, imposed by accelerated internalization. This is advantageous because it would prevent internalized receptors from flooding the lysosomal sorting machinery, which is known to be rate limiting (Herbst et al., 1994; Opresko et al., 1995). 679-LL-mediated intracellular retention, however, constitutes the predominant mechanism for sorting to lysosomes. Since E3-13.7 does not promote increased rates of EGFR internalization (Hoffman and Carlin, 1994), this would explain why protein ubiquitylation is not required for adenovirus-induced downregulation. The fact that 679-LL-mediated intracellular retention is necessary for E3-13.7-dependent downregulation suggests this dileucine motif supports the same lysosomal sorting function in adenovirus-infected and ligand-stimulated cells.

EGFR is the only ERBB receptor that is efficiently downregulated following ligand stimulation. Other ERBB receptors are either defective for internalization or for sorting to lysosomes. EGFR and ERBB2 both recruit and activate CBL (Waterman and Yarden, 2001), and all four ERBB receptors have a conserved tyrosine-based signal that has also been implicated in lysosomal sorting (Jones et al., 2002; Kurten et al., 1996). By contrast, the 679-LL signal is not conserved in any of the other ERBB receptors (Kil et al., 1999) (Table 1b). This suggests that 679-LL has a key role in fine-tuning EGFR-dependent cell-signaling by controlling threshold levels of EGFR sorting to lysosomes.

The authors wish to thank Nick Cianciola, Sean Ryan, and Ankur Shah for many helpful discussions. Dedicated to our colleague and friend Cheng He. This work was supported by Public Health Service grants RO1 GM64243 and P50 DK54178 to C.C.

References

Alwan, H. A., van Zoelen, E. J. J. and van Leeuwen, J. E. M. (2003). Ligand-induced lysosomal epidermal growth factor receptor (EGFR) degradation is preceded by proteasome-dependent EGFR de-ubiquitination. *J. Biol. Chem.* **278**, 35781-35790.

Amerik, A. Y., Nowak, J., Swaminathan, S. and Hochstrasser, M. (2000). The Doa4 deubiquitinating enzyme is functionally linked to the vacuolar protein-sorting and endocytic pathways. *Mol. Biol. Cell* **11**, 3365-3380.

Andersen, N. H. and Tong, H. (1997). Empirical parameterization of a model for predicting peptide helix/coil equilibrium populations. *Protein Sci.* **6**, 1920-1936.

Aniento, F., Gu, F., Parton, R. and Gruenberg, J. (1996). An endosomal βCOP is involved in the pH-dependent formation of transport vesicles destined for late endosomes. *J. Cell Biol.* **133**, 29-41.

Authier, F. and Chauvet, G. (1999). In vitro endosome-lysosome transfer of dephosphorylated EGF receptor and Shc in rat liver. *FEBS Lett.* **461**, 25-31.

Baass, P. C., DiGuglielmo, G. M., Authier, F., Posner, B. I. and Bergeron, J. J. M. (1995). Compartmentalized signal transduction by receptor tyrosine kinases. *Trends Cell Biol.* **5**, 465-470.

Baulida, J., Kraus, M. H., Alimandi, M., Fiore, P. P. D. and Carpenter, G. (1996). All ErbB receptors other than the epidermal growth factor receptor are endocytosis impaired. *J. Biol. Chem.* **271**, 5251-5257.

Blume-Jensen, P. and Hunter, T. (2001). Oncogenic kinase signalling. *Nature* **411**, 355-365.

Bonifacino, J. S. (2004). The GGA proteins: adaptors on the move. *Nat. Rev. Mol. Cell Biol.* **5**, 23-32.

Bonifacino, J. S. and Weissman, A. M. (1998). Ubiquitin and the control of protein fate in the secretory and endocytic pathways. *Annu. Rev. Cell Dev. Biol.* **14**, 19-57.

Bonifacino, J. and Traub, L. (2003). Signals for sorting of transmembrane proteins to endosomes and lysosomes. *Annu. Rev. Biochem.* **72**, 395-457.

Bonifacino, J. S. and Dell'Angelica, E. C. (1999). Molecular bases for the recognition of tyrosine-based sorting signals. *J. Cell Biol.* **145**, 923-926.

Bowtell, D. D. and Langdon, W. Y. (1995). The protein product of the c-cbl oncogene rapidly complexes with the EGF receptor and is tyrosine phosphorylated following EGF stimulation. *Oncogene* **11**, 1561-1567.

Carlin, C. R. and Knowles, B. B. (1984). Biosynthesis of the epidermal growth factor receptor in human epidermoid carcinoma-derived A431 cells. *J. Biol. Chem.* **259**, 7902-7908.

Carlin, C. R., Tollefson, A. E., Brady, H. A., Hoffman, B. L. and Wold, W. (1989). Epidermal growth factor receptor is down-regulated by a 10,400 MW protein encoded by the E3 region of adenovirus. *Cell* **57**, 135-144.

Carpenter, G. (2000). The EGF receptor: a nexus for trafficking and signaling. *BioEssays* **22**, 697-707.

Ceresa, B. P. and Schmid, S. L. (2000). Regulation of signal transduction by endocytosis. *Curr. Opin. Cell Biol.* **12**, 204-210.

Choowongkomen, K., Carlin, C. R. and Sönnichsen, F. D. (2005). A structural model for the membrane-bound form of the juxtamembrane domain of the epidermal growth factor receptor. *J. Biol. Chem.* **280**, 24043-24052.

Clague, M. J. and Urbe, S. (2001). The interface of receptor trafficking and signalling. *J. Cell Sci.* **114**, 3075-3081.

Crivici, A. and Ikura, M. (1995). Molecular and structural basis of target recognition by calmodulin. *Annu. Rev. Biophys. Biomol. Struct.* **24**, 85-116.

Crooks, D., Kil, S. J., McCaffery, J. M. and Carlin, C. (2000). E3-13.7 integral membrane proteins encoded by human adenoviruses alter epidermal growth factor receptor trafficking by interacting directly with receptors in early endosomes. *Mol. Biol. Cell* **11**, 3559-3572.

de Melker, A. A., van der Horst, G., Calafat, J., Jansen, H. and Borst, J. (2001). c-Cbl ubiquitinates the EGF receptor at the plasma membrane and remains receptor associated throughout the endocytic route. *J. Cell Sci.* **114**, 2167-2178.

de Melker, A., van der Horst, G. and Borst, J. (2004). Ubiquitin ligase activity of c-Cbl guides the EGF receptor into clathrin-coated pits by two distinct modes of Eps15 recruitment. *J. Biol. Chem.* **279**, 55465-55473.

DiFiore, P. P. and Gill, G. N. (1999). Endocytosis and mitogenic signaling. *Curr. Opin. Cell Biol.* **11**, 483-488.

Dupre, S. and Haguenauer-Tsapis, R. (2001). Deubiquitination step in the endocytic pathway of yeast plasma membrane proteins: Crucial role of Doa4p ubiquitin isopeptidase. *Mol. Cell. Biol.* **21**, 4482-4494.

Fleishman, S. J., Schlessinger, J. and Ben-Tal, N. (2002). A putative molecular-activation switch in the transmembrane domain of erbB2. *Proc. Natl. Acad. Sci. USA* **99**, 15937-15940.

Futter, C. E., Pearse, A., Hewlett, L. J. and Hopkins, C. R. (1996). Multivesicular endosomes containing internalized EGF-EGF receptor complexes mature and then fuse directly with lysosomes. *J. Cell Biol.* **132**, 1011-1023.

Grovdal, L., Stang, E., Sorkin, A. and Madshus, I. H. (2004). Direct interaction of Cbl with pTyr 1045 of the EGF receptor (EGFR) is required to sort the EGFR to lysosomes for degradation. *Exp. Cell Res.* **300**, 388-395.

Gu, F., Aniento, F., Parton, R. G. and Gruenberg, J. (1997). Functional dissection of COP-I subunits in the biogenesis of multivesicular bodies. *J. Cell Biol.* **139**, 1183-1195.

Haglund, K., Shimokawa, N., Szymkiewicz, I. and Dikic, I. (2002). Cbl-directed monoubiquitination of CIN85 is involved in regulation of ligand-induced degradation of EGF receptors. *Proc. Natl. Acad. Sci. USA* **99**, 12191-12196.

Herbst, J. J., Opresko, L. K., Walsh, B. J., Lauffenberger, D. A. and Wiley, H. S. (1994). Regulation of post-endocytic trafficking of the epidermal growth factor receptor through endosomal retention. *J. Biol. Chem.* **269**, 12865-12873.

Hershko, A. and Ciechanover, A. (1998). The ubiquitin system. *Annu. Rev. Biochem.* **67**, 425-479.

Hilgendorf, A., Lindberg, J., Ruzsics, Z., Honing, S., Elsing, A., Lofqvist, M., Engelmann, H. and Burgert, H.-G. (2003). Two distinct transport motifs in the adenovirus E3 proteins act in concert to down-modulate apoptosis receptors and the epidermal growth factor receptor. *J. Biol. Chem.* **278**, 51872-51884.

Hoellerer, M., Noble, M., Labesse, G., Campbell, I., Werner, J. and Arold, S. (2003). Molecular recognition of paxillin LD motifs by the focal adhesion targeting domain. act in concert to down-modulate apoptosis receptors and the epidermal growth factor *Structure* **11**, 1207-1217.

Hoffman, B. L., Ullrich, A., Wold, W. and Carlin, C. (1990). Retrovirus-mediated transfer of an adenovirus gene encoding an integral membrane protein is sufficient to down regulate the receptor for epidermal growth factor. *Mol. Cell. Biol.* **10**, 5521-5524.

Hoffman, P. and Carlin, C. (1994). Adenovirus E3 protein causes constitutively internalized EGF receptors to accumulate in a prelysosomal compartment, resulting in enhanced degradation. *Mol. Cell. Biol.* **14**, 3695-3706.

Hoffman, P., Yaffe, M. B., Hoffman, B. L., Yei, S., Wold, W. S. M. and Carlin, C. (1992a). Characterization of the adenovirus E3 protein that down-regulates the epidermal growth factor receptor. *J. Biol. Chem.* **267**, 13480-13487.

Hoffman, P. H., Rajakumar, P., Hoffman, B., Heuertz, R., Wold, W. S. M. and Carlin, C. R. (1992b). Evidence for intracellular down-regulation of the epidermal growth factor receptor during adenovirus infection by an EGF-independent mechanism. *J. Virol.* **66**, 197-203.

Hopkins, C. (1983). Intracellular routing of transferrin and transferrin receptors in epidermoid carcinoma A431 cells. *Cell* **35**, 321-330.

Hurley, J. H. (2003). Leucine in the sky with diamonds. *Structure* **10**, 1192-1193.

Hurley, J. H., Anderson, D. E., Beach, B., Canagarajah, B., Jonathan Ho, Y. S., Jones, E., Miller, G., Misra, S., Pearson, M., Saidi, L. et al. (2002). Structural genomics and signaling domains. *Trends Biochem. Sci.* **27**, 48-53.

Joazeiro, C. A. P., Wing, S. S., Huang, H., Leverson, J. D., Hunter, T. and Liu, Y. (1999). The tyrosine kinase negative regulator c-Cbl as a RING-type, E2-dependent ubiquitin-protein ligase. *Science* **286**, 309-312.

Jones, S. M., Foreman, S. K., Shank, B. B. and Kurten, R. C. (2002). EGF receptor downregulation depends on a trafficking motif in the distal tyrosine kinase domain. *Am. J. Physiol. Cell Physiol.* **282**, C420-C433.

Katzmann, D. J., Babst, M. and Emr, S. D. (2001). Ubiquitin-dependent sorting into the multivesicular body pathway requires the function of a conserved endosomal protein sorting complex, ESCRT-I. *Cell* **106**, 145-155.

Kil, S. and Carlin, C. (2000). EGF receptor residues Leu^{679}, Leu^{680} mediate selective sorting of ligand-receptor complexes in early endocytic compartments. *J. Cell. Physiol.* **185**, 47-60.

Kil, S. J., Hobert, M. E. and Carlin, C. (1999). A leucine-based determinant in the EGF receptor juxtamembrane domain is required for the efficient transport of ligand-receptor complexes to lysosomes. *J. Biol. Chem.* **274**, 3141-3150.

Kim, H. and Muller, W. J. (1999). The role of the epidermal growth factor receptor family in mammary tumorigenesis and metastasis. *Exp. Cell Res.* **253**, 78-87.

Kurten, R. C., Cadena, D. L. and Gill, G. N. (1996). Enhanced degradation of EGF receptors by a sorting nexin, SNX1. *Science* **272**, 1008-1110.

Laemmli, U. K. (1970). Cleavage of structural proteins during the assembly of the head of bacteriophage T4. *Nature* **227**, 680-685.

Lando, Z., Sarin, P., Megson, M., Greene, W. C., Waldman, T. A., Gallo, R. C. and Broder, S. (1983). Association of human T-cell leukaemia/lymphoma virus with the Tac antigen marker for the human T-cell growth factor receptor. *Nature* **305**, 733-736.

Lauterwein, J., Bosch, C., Brown, L. R. and Wuthrich, K. (1979). Physicochemical studies of the protein-lipid interactions in melittin-containing micelles. *Biochim. Biophys. Acta* **556**, 244-264.

Lefkowitz, G., Waterman, H., Ettenberg, S. A., Katz, M., Tsygankov, A. Y., Alroy, I., Lavi, S., Iwai, K., Reiss, Y., Ciechanover, A. et al. (1999). Ubiquitin ligase activity and tyrosine phosphorylation underlie suppression of growth factor signaling by c-Cbl/Sli-1. *Mol. Cell* **4**, 1029-1040.

Lenferink, A., Pinkas-Kramarski, R., van de Poll, M., van Vugt, M., Klapper, L., Tzahar, E., Waterman, H., Sela, M., van Zoelen, E. and Yarden, Y. (1998). Differential endocytic routing of homo- and hetero-dimeric ErbB tyrosine kinases confers signaling superiority to receptor heterodimers. *EMBO J.* **17**, 3385-3397.

Levkowitz, G., Waterman, H., Zamir, E., Kam, Z., Oved, S., Langdon, W., Beguinot, L., Geiger, B. and Yarden, Y. (1999). c-Cbl/Sli-1 regulates endocytic sorting and ubiquitination of the epidermal growth factor receptor. *Genes Dev.* **12**, 3663-3674.

Lill, N. L., Douillard, P., Awwad, R. A., Ota, S., Lupher, M. L., Jr, Miyake, S., Meissner-Lula, N., Hsu, V. W. and Band, H. (2000). The evolutionarily conserved N-terminal region of Cbl is sufficient to enhance down-regulation of the epidermal growth factor receptor. *J. Biol. Chem.* **275**, 367-377.

Lindberg, M., Biverstahl, H., Graslund, A. and Maler, L. (2003). Structure and positioning comparison of two variants of penetratin in two different membrane mimicking systems by NMR. *Eur. J. Biochem.* **270**, 3055-3063.

Losko, S., Kopp, F., Kranz, A. and Kölling, R. (2001). Uptake of the ATP-binding cassette (ABC) transporter Ste6 into the yeast vacuole is blocked in the doa4 mutant. *Mol. Biol. Cell* **12**, 1047-1059.

Marmor, M. D. and Yarden, Y. (2004). Role of protein ubiquitylation in regulating endocytosis of receptor tyrosine kinases. *Oncogene* **15**, 2057-2070.

Miller, K., Beardmore, J., Kanely, H., Schlessinger, J. and Hopkins, C. R. (1986). Localization of the EGF receptor within the endosome of EGF-stimulated A431 cells. *J. Cell Biol.* **102**, 500-509.

Mukherjee, S., Ghosh, R. N. and Maxfield, F. R. (1997). Endocytosis. *Physiol. Rev.* **77**, 759-803.

Neve, R. M., Lane, H. A. and Hynes, N. E. (2001). The role of overexpressed HER2 in transformation. *Ann. Oncol.* **12**, S9-S13.

Opresko, L. K., Chang, C. P., Will, B. H., Burke, P. M., Gill, G. N. and Wiley, H. S. (1995). Endocytosis and lysosomal targeting of epidermal growth factor receptors are mediated by distinct sequences independent of the tyrosine kinase domain. *J. Biol. Chem.* **270**, 4325-4333.

Piotto, M., Saudek, V. and Sklenar, V. (1992). Gradient-tailored excitation for single-quantum NMR spectroscopy of aqueous solutions. *J. Biomol. NMR* **2**, 661-665.

Piper, R. C. and Luzio, J. P. (2001). Late endosomes: sorting and partitioning in multivesicular bodies. *Traffic* **2**, 612-621.

Pruss, R. M. and Herschman, H. R. (1977). Variants of 3T3 cells lacking mitogenic response to epidermal growth factor. *Proc. Natl. Acad. Sci. USA* **74**, 3918-3921.

Sachse, M., Urbe, S., Oorschot, V., Strous, G. J. and Klumperman, J. (2002). Bilayered clathrin coats on endosomal vacuoles are involved in protein sorting toward lysosomes. *Mol. Biol. Cell* **13**, 1313-1328.

Schlessinger, J. (2000). Cell signaling by receptor tyrosine kinases. *Cell* **103**, 211-225.

Smit, L., van der Horst, G. and Borst, J. (1996). Formation of Shc/Grb2- and Crk adaptor complexes containing tyrosine phosphorylated Cbl upon stimulation of the B-cell antigen receptor. *Oncogene* **13**, 381-389.

Sorkin, A. (2000). The endocytosis machinery. *J. Cell Sci.* **113**, 4375-4376.

Sorkin, A. and Von Zastrow, M. (2002). Signal transduction and endocytosis: close encounters of many kinds. *Nat. Rev. Mol. Cell Biol.* **3**, 600-614.

Stamos, J., Sliwkowski, M. X. and Eigenbrot, C. (2002). Structure of the epidermal growth factor receptor kinase domain alone and in complex with a 4-anilinoquinazoline inhibitor. *J. Biol. Chem.* **277**, 46265-46272.

Teis, D. and Huber, L. (2003). The odd couple: signal transduction and endocytosis. *Cell Mol. Life Sci.* **60**, 2020-2033.

Towbin, H., Staehelin, T. and Gordon, J. (1979). Electrophoretic transfer of proteins from polyacrylamide gels to nitrocellulose sheets: procedure and some applications. *Proc. Natl. Acad. Sci. USA* **76**, 4350-4354.

Vinogradova, O., Carlin, C. R., Sonnichsen, F. D. and Sanders, C. R. (1998). A membrane setting for the sorting motifs present in the adenovirus E3-13.7 protein which down-regulates the epidermal growth factor receptor. *J. Biol. Chem.* **273**, 17343-17350.

Wang, Z., Zhang, L., Yeung, T. K. and Chen, X. (1999). Endocytosis deficiency of epidermal growth factor (EGF) receptor-ErbB2 heterodimers in response to EGF stimulation. *Mol. Biol. Cell* **10**, 1621-1636.

Waterman, H., Sabanai, I., Geiger, B. and Yarden, Y. (1998). Alternative intracellular routing of ErbB receptors may determine signaling potency. *J. Biol. Chem.* **273**, 13819-13827.

Waterman, H. and Yarden, Y. (2001). Molecular mechanisms underlying endocytosis and sorting of ErbB receptors. *FEBS Lett.* **490**, 142-152.

Wiley, H. S. (1988). Anomolous binding of epidermal growth factor to A431 cells is due to the effect of high receptor densities and a saturable endocytic system. *J. Cell Biol.* **107**, 801-810.

Wiley, H. S. (2003). Trafficking of the ErbB receptors and its influence on signaling. *Exp. Cell Res.* **284**, 78-88.

Wiley, H. S. and Burke, P. M. (2001). Regulation of receptor tyrosine kinase signaling by endocytic trafficking. *Traffic* **2**, 12-18.

Wishart, D. S., Sykes, B. D. and Richards, F. M. (1992). The chemical shift index: a fast and simple method for the assignment of protein secondary structure through NMR spectroscopy. *Biochemistry* **31**, 1647-1651.

Worthylake, R., Opresko, L. K. and Wiley, H. S. (1999). ErbB-2 amplification inhibits down-regulation and induces constitutive activation of both erbB-2 and epidermal growth factor receptors. *J. Biol. Chem.* **274**, 8865-8874.